Year : 2015

Dying neurons in thalamus of asphyxiated term newborns and rats are autophagic

Pittet Marie Pascale

UNIVERSITE DE LAUSANNE - FACULTE DE BIOLOGIE ET DE MEDECINE

Département des Neurosciences Fondamentales

Dying neurons in thalamus of asphyxiated term newborns and rats are autophagic

THESE

préparée sous la direction du Docteure Anita C. Truttmann, PD et MER
(avec la co-direction du Docteur PhD Julien P. Puyal, MER)

et présentée à la Faculté de biologie et de médecine de
l'Université de Lausanne pour l'obtention du grade de

DOCTEUR EN MEDECINE

par

Marie Pascale PITTET

Médecin diplômée de la Confédération Suisse
Originaire de Sâles (FR)

Lausanne

2015

UNIL | Université de Lausanne

Faculté de biologie et de médecine

Ecole Doctorale
Doctorat en médecine

Imprimatur

Vu le rapport présenté par le jury d'examen, composé de

Directeur de thèse	*Madame la Docteure* ***Anita Truttmann***
Co-Directeur de thèse	*Monsieur le Docteur* ***Julien Puyal***
Expert	*Madame la Professeure* ***Lee Laurent-Applegate***
Directrice de l'Ecole doctorale	*Madame la Professeure* ***Stephanie Clarke***

la Commission MD de l'Ecole doctorale autorise l'impression de la thèse de

Madame Marie Pascale Pittet

intitulée

Dying neurons in thalamus of asphyxiated term newborns and rats are autophagic

Lausanne, le 17 février 2015

pour Le Doyen
de la Faculté de Biologie et de Médecine

Madame la Professeure Stephanie Clarke
Directrice de l'Ecole doctorale

Rapport de Synthèse

Enjeu: Déterminer si la macroautophagie est activée de façon excessive dans les neurones en souffrance dans l'encéphalopathie anoxique-ischémique du nouveau-né à terme.
Contexte de la recherche: L'encéphalopathie anoxique-ischémique suite à une asphyxie néonatale est associée à une morbidité neurologique à long terme. Une diminution de son incidence reste difficile, son primum movens étant soudain, imprévisible voire non identifiable. Le développement d'un traitement pharmacologique neuroprotecteur post-anoxie reste un défi car les mécanismes impliqués dans la dégénérescence neuronale sont multiples, interconnectés et encore insuffisamment compris. En effet, il ressort des études animales que la notion dichotomique de mort cellulaire apoptotique (type 1)/nécrotique (type 3) est insuffisante. Une même cellule peut présenter des caractéristiques morphologiques mixtes non seulement d'apoptose et de nécrose mais aussi parfois de mort autophagique (type 2) plus récemment décrite. L'autophagie est un processus physiologique normal et essentiel de dégradation de matériel intracellulaire par les enzymes lysosomales. La macroautophagie, nommée simplement autophagie par la suite, consiste en la séquestration de parties de cytosol à éliminer (protéines et organelles) dans des compartiments intermédiaires, les autophagosomes, puis en leur fusion avec des lysosomes pour former des autolysosomes. Dans certaines conditions de stress telles que l'hypoxie et l'excitoxicité, une activité autophagique anormalement élevée peut être impliquée dans la mort cellulaire soit comme un mécanisme de mort indépendant (autodigestion excessive correspondante à la mort cellulaire de type 2) soit en activant d'autres voies de mort comme celles de l'apoptose.
Description de l'article: Ce travail examine la présence de l'autophagie et son lien avec la mort cellulaire dans les neurones d'une région cérébrale fréquemment atteinte chez le nouveau-né humain décédé après une asphyxie néonatale sévère, le thalamus ventro-latéral. Ces résultats ont été comparés à ceux obtenus dans un modèle d'hypoxie-ischémie cérébrale chez le raton de 7 jours (dont le cerveau serait comparable à celui d'un nouveau-né humain de 34-37 semaines de gestation). Au total 11 nouveau-nés à terme décédés peu après la naissance ont été rétrospectivement sélectionnés, dont 5 présentant une encéphalopathie hypoxique-ischémique sévère et 6 décédés d'une cause autre que l'asphyxie choisis comme cas contrôle. L'autophagie et l'apoptose neuronale ont été évaluées sur la base d'une étude immunohistochimique et d'imagerie confocale de coupes histologiques en utilisant des marqueurs tels que LC3 (protéine dont la forme LC3-II est liée à la membrane des autophagosomes), p62/SQSTM1 (protéine spécifiquement dégradée par autophagie), LAMP1 (protéine membranaire des lysosomes et des autolysosomes), Cathepsin D ou B (enzymes lysosomales), TUNEL (détection de la fragmentation de l'ADN se produisant lors de l'apoptose), CASPASE-3 activée (protéase effectrice de l'apoptose) et PGP9.5 (protéine spécifique aux neurones). Chez le raton l'étude a pu être étendue en utilisant d'autres méthodes complémentaires telles que la microscopie électronique et le Western-blot. Une quantification des différents marqueurs montre une augmentation statistiquement significative de l'autophagie neuronale dans les cas d'asphyxie par rapport aux cas contrôles chez l'humain comme chez le raton. En cas d'asphyxie, les mêmes neurones expriment une densité accrue d'autophagosomes et d'autolysosomes par rapport aux cas contrôles. De plus, les neurones hautement autophagiques présentent des caractéristiques de l'apoptose.
Conclusion: Cette étude montre, pour la première fois, que les neurones thalamiques lésés en cas d'encéphalopathie hypoxique-ischémique sévère présentent un niveau anormalement élevé d'activité autophagique comme démontré chez le raton hypoxique-ischémique. Ce travail permet ainsi de mettre en avant l'importance de considérer l'autophagie comme acteur dans la mort neuronale survenant après asphyxie néonatale.
Perspectives: Récemment un certain nombre d'études in vitro ou sur des modèles d'ischémie cérébrale chez les rongeurs suggèrent un rôle important de la macroautophagie dans la mort neuronale. Ainsi, l'inhibition spécifique de la macroautophagie devrait donc être envisagée dans le futur développement des stratégies neuroprotectrices visant à protéger le cerveau des nouveau-nés à terme suite à une asphyxie.

RESEARCH ARTICLE

Dying Neurons in Thalamus of Asphyxiated Term Newborns and Rats Are Autophagic

Vanessa Ginet, PhD,[1]* Marie P. Pittet, MD,[1,2]* Coralie Rummel,[1] Maria Chiara Osterheld, MD,[3] Reto Meuli, MD, PhD,[4] Peter G. H. Clarke, PhD,[1] Julien Puyal, PhD[1,2&], and Anita C. Truttmann, MD[2&]

Objective: Neonatal hypoxic–ischemic encephalopathy (HIE) still carries a high burden by its mortality and long-term neurological morbidity in survivors. Apart from hypothermia, there is no acknowledged therapy for HIE, reflecting the lack of mechanistic understanding of its pathophysiology. (Macro)autophagy, a physiological intracellular process of lysosomal degradation, has been proposed to be excessively activated in excitotoxic conditions such as HIE. The present study examines whether neuronal autophagy in the thalamus of asphyxiated human newborns or P7 rats is enhanced and related to neuronal death processes.
Methods: Neuronal autophagy and cell death were evaluated in the thalamus (frequently injured in severe HIE) of both human newborns who died after severe HIE (n = 5) and P7 hypoxic–ischemic rats (Rice–Vannuci model). Autophagic (LC3, p62), lysosomal (LAMP1, cathepsins), and cell death (TUNEL, caspase-3) markers were studied by immunohistochemistry in human and rat brain sections, and by additional methods in rats (immunoblotting, histochemistry, and electron microscopy).
Results: Following severe perinatal asphyxia in both humans and rats, thalamic neurons displayed up to 10-fold ($p < 0.001$) higher numbers of autophagosomes and lysosomes, implying an enhanced autophagic flux. The highly autophagic neurons presented strong features of apoptosis. These findings were confirmed and elucidated in more detail in rats.
Interpretation: These results show for the first time that autophagy is enhanced in severe HIE in dying thalamic neurons of human newborns, as in rats. Experimental neuroprotective strategies targeting autophagy could thus be a promising lead to follow for the development of future therapeutic approaches.

ANN NEUROL 2014;76:695–711

Perinatal asphyxia is a major cause of newborn mortality and long-term neurodevelopmental disabilities, with very limited therapeutic options.[1] Its best known complication is hypoxic–ischemic encephalopathy (HIE), which is characterized by acute neurological impairment, often with seizures and early lesions seen on magnetic resonance imaging (MRI), especially at the level of the perirolandic cortex, the basal ganglia, the thalamus, and the brainstem. Twenty-five percent of HIE cases lead to death in the first week of life, and up to 50% of survivors develop permanent sequelae such as cerebral palsy, seizures, and cognitive and neurosensorial impairment.[2] Despite considerable efforts in research to find clinically safe and effective neuroprotective pharmacotherapy, the only therapy that is currently approved is moderate hypothermia. The heterogeneity of the human hypoxic–ischemic insults and the presence of multiple interacting cell death mechanisms are major difficulties.

Our current understanding of neuronal cell death in human HIE term newborns is very limited because of the lack of human brain studies.[3] One of the most relevant animal models in HIE is a combination of unilateral

View this article online at wileyonlinelibrary.com. DOI: 10.1002/ana.24257

Received Jun 3, 2013, and in revised form Aug 19, 2014. Accepted for publication Aug 19, 2014.

Address correspondence to Dr Truttmann, Clinic of Neonatology, University Hospital Center and University of Lausanne, Department of Pediatrics and Pediatric Surgery, Avenue Pierre Decker, Maternité, Lausanne, Vaud, Switzerland 1011. E-mail: anita.truttmann@chuv.ch

From the [1]Department of Fundamental Neurosciences, University of Lausanne; [2]Clinic of Neonatology, Department of Pediatrics, University Hospital Center; [3]Institute of Pathology, University Hospital Center and University of Lausanne; and [4]Department of Diagnostic and Interventional Radiology, University Hospital Center and University of Lausanne, Lausanne, Switzerland.

*V. Gine and M. P. Pittet contributed equally to this article.
[&]Share senior authorship.

common carotid artery ligation and exposure to hypoxia in P7 rats,[4] this age being considered comparable to late preterm/term in human brains (34–36 weeks gestation).[5,6] An important conclusion emerging from studies on rodent perinatal hypoxia–ischemia (HI) is that cell death occurs along an apoptotic–necrotic "continuum"[7] involving predominance of hybrid morphologies of cell death with mixed features of apoptosis and necrosis.[8] However, these may not be the only cell death mechanisms involved, because morphological characteristics of enhanced autophagy have recently been described in the dying neurons.[9–11]

Macroautophagy (hereafter called autophagy) is a physiological degradative process in which cellular components are sequestered in autophagosomes, which fuse with acidic organelles (late endosomes, lysosomes, etc) to form autolysosomes containing the hydrolytic enzymes necessary for the autophagic degradation. Autophagy is essential for maintaining homeostasis and cell survival, but recent studies indicate that it can be involved in cell death, either as a trigger of apoptosis or necrosis, or as an independent mechanism of cell death.[12]

In situations of cerebral HI, the evidence for a death-mediating role of autophagy stems from a combination of morphological and functional evidence. Different studies have demonstrated the presence of enhanced autophagy in dying neurons in neonatal animal models of cerebral ischemia or HI in the cortex and/or hippocampus.[9,10,13] Inhibition of autophagy either pharmacologically[14] or more specifically in neonatal conditional knockout mice with neuron-specific deletion of *Atg7*[10] is neuroprotective, suggesting a death-mediating role of autophagy.

As the thalamus, including its ventrolateral nucleus (VLNT), is often involved in human HIE, we have studied whether neuronal autophagy is enhanced in the VLNT in brains of human newborns who died from severe HIE and have compared the results with those obtained in a human control group and in the animal model.

Materials and Methods

Rat Model of Neonatal HI

All experiments were performed in accordance with the Swiss laws for the protection of animals and were approved by the Vaud Cantonal Veterinary Office. Seven-day-old male rats (Sprague Dawley; Janvier Labs, Saint Berthevin, France) underwent HI (8% of oxygen for 2 hours) according to the Rice–Vannucci model[4] as previously described.[9] The damage induced by our model of neonatal cerebral HI (2 hours of hypoxia) was very severe, but with low individual/litter variability in our hands compared to shorter and less severe hypoxic periods (Fig 1A, B).

Human Newborn Brain Specimens

Human brain tissues were obtained from 11 deceased and autopsied newborns, provided by the Institute of Pathology, University of Lausanne (Table 1). The studied population was selected retrospectively from the death reports of the Clinic of Neonatology (Lausanne University Hospital) between 2001 and 2009. Autopsies were done for medical and legal reasons, and informed consent was obtained from the parents. The postmortem interval (time between death and autopsy) was between 5 and 24 hours, and the bodies where conserved in a cold environment. During autopsy, the brain was removed and fixed in 10% buffered formalin for 3 weeks. Samples were then embedded in paraffin, and 3μm-thick sections were cut. Specimens were then anonymized for research purposes with the approval of the local ethical committee. We selected newborns who had died after birth in the context of severe HIE (HIE group, n = 5). Death was due to withdrawal of care in 4 cases and due to additional respiratory failure in 1 case. The criteria for HIE cases were: newborns at or near term (35–37 weeks gestation), with severe perinatal asphyxia, and clinical HIE according to Sarnat grade III.[15] For the control group (n = 6), newborns at or near term (35–37 weeks of gestation) with life-incompatible conditions were selected (transposition of the great vessels with intact septum [n = 1], primary pulmonary lymphangiectasia [n = 1], congenital diaphragmatic hernia [n = 1], congenital myopathy [n = 2], intrauterine demise with endocardial fibroelastosis [n = 1]). Babies with cerebral malformations and genetic anomalies were excluded, as well as babies from whom autoptic material from thalamus was no longer available. For comparing the selection criteria between the groups, we calculated the resuscitation score according to Miller et al.[16]

Cerebral MRI and Apparent Diffusion Coefficient

MRI was available for 3 of 5 HIE cases, using 1.5 or 3T scanners. Conventional T1 and T2 images and diffusion-weighted images (DWI) were acquired using spin echo echoplanar imaging, with 5mm-thick slices (b values: 0, 500, 1,000mm^2/s). Apparent diffusion coefficient (ADC) values were calculated from the ADC map choosing similar bilateral regions of interest in the VLNT. As reference values, we used those published by Rutherford et al.[17]

Immunoblotting

Immunoblots on thalamic extracts of sham-operated or HI rat pups were done as described previously.[18] The following primary antibodies were used for protein immunodetection: anti–α-tubulin (sc-8035) mouse monoclonal from Santa Cruz Biotechnology (Santa Cruz, CA); anti-LC3 (ab48394) rabbit polyclonal from Abcam (Cambridge, MA); anti–active caspase-3 (9661) from Cell Signaling Technology (Danvers, MA); anti–p62/SQSTM1 (P0067) rabbit polyclonal from Sigma-Aldrich (St Louis, MO), and anti-fodrin (FG6090) mouse monoclonal

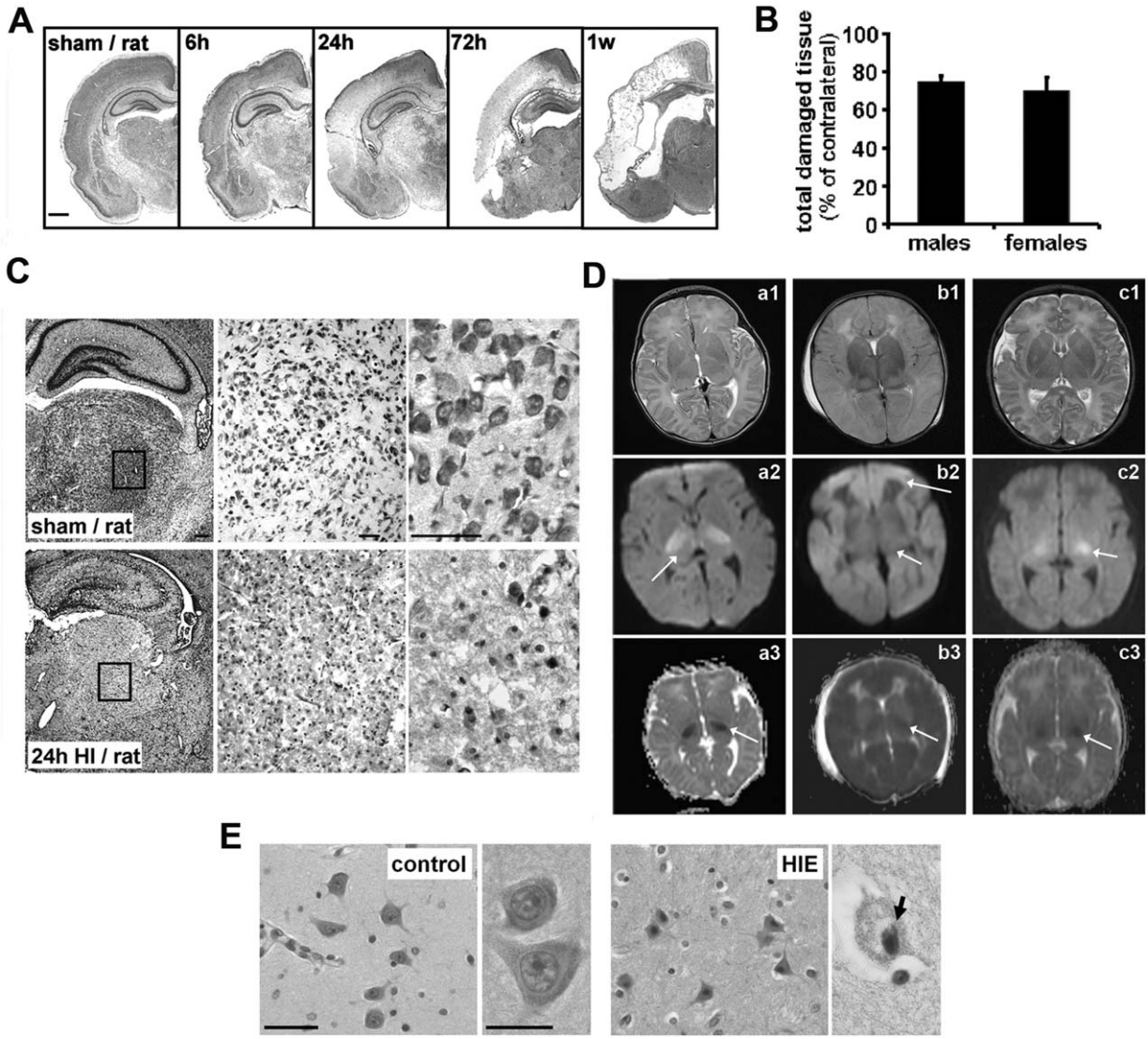

FIGURE 1: Perinatal asphyxia induces severe neuronal injury in the thalamus of both rat and human neonates. (A) Representative images of coronal brain sections stained with cresyl violet showing the evolution of the lesion as sampled at 4 time-points: 6 hours, 24 hours, 72 hours, and 1 week after hypoxia-ischemia (HI). Bar = 1cm. (B) Quantification of damaged brain tissue 24 hours after the insult induced by 2 hours of hypoxia in P7 male and female rats shows a severe but reproducible lesion. No significant difference in the percentage of total damaged tissue relative to the contralateral hemisphere was found between males (74 ± 4%, n = 11) and females (70 ± 8%, n = 11). Values are mean ± standard deviation. (C) Hematoxylin–eosin (HE) stains reveal that the rat ventrobasal thalamus is strongly affected by perinatal HI 24 hours after the insult, with the presence of cell shrinkage and pyknotic nuclei. Black rectangles correspond to the higher magnifications in the ventrobasal thalamus. Bars = 200μm for low resolution (left panel) and 50μm for higher magnifications (middle and right panels). (D) Cerebral magnetic resonance imaging with T2-weighted, diffusion, and apparent diffusion coefficient (ADC) maps obtained in hypoxic–ischemic encephalopathy (HIE) Cases 1 (a1–3), 2 (b1–3), and 3 (c1–3). Top row shows transverse T2-weighted images at 34 hours (a), 40 hours (b), and 48 (c) hours after birth, respectively; middle row shows the diffusion-weighted images (DWIs) at the same times; and bottom row represents the ADC maps. Image a1 shows the absence of signal anomaly in thalamus, basal ganglia, and cortex on T2-weighted images, but a2 presents a restricted diffusion in thalamus *(arrow)* bilaterally as well as the corticospinal tract and both hippocampi (not seen here), confirmed on ADC maps (*arrow* in a3). Image b1 shows a severe diffuse cerebral edema with hyperintensity in thalamus/basal ganglia and loss of differentiation between gray and white matter for global cortex, seen also on the DWI (b2) with restricted diffusion on the thalamus *(short arrow)* and global cortex *(long arrow)* and confirmed on ADC maps (b3). Image c1 shows no anomaly on this image, but additional corticospinal tract hyperintensities were seen on adjacent images. Image c2 shows restricted diffusion bilaterally in the posterior limb of the internal capsule and ventrolateral thalamus; restricted diffusion occurred also in the corticospinal tract (not in this image, but in adjacent ones). This was confirmed on ADC maps (c3). The mean ADC values measured on the right and left ventrolateral nucleus of the thalamus (VLNT) were strongly reduced in all 3 HIE cases, confirming cytotoxic edema in VLNT bilaterally. (E) Representative images showing that dying neurons in the VLNT of HIE cases display cell shrinkage and pyknotic nuclei as shown using an HE stain compared to control cases. Bar = 20μm.

TABLE 1. Descriptive Data of the Human Population

Groups	HIE, n = 5	Control, n = 6	*p*
Gestational age, days			0.712
Median	277	272.5	
Range	268–287	250–290	
Birth weight, g			0.537
Median	3,180	3,255	
Range	2,610–3440	2,240–4,070	
Apgar, 1 min			0.029[a]
Median	0	2[b]	
Range	0–1	1–7	
Apgar, 10 min			0.673
Median	4	5[b]	
Range	1–6	0–8	
Umbilical arterial pH			0.019[a]
Median	6.83	7.28[b]	
Range	6.7–6.99	7.23–7.32	
Lactate, mmol/l			0.596
Median	17	16[b]	
Range	16–21	3–21	
Time of death after birth, h			0.143
Median	44	13[b]	
Range	20–171	1–672	
Resuscitation score[c]			0.600
Median	6	6[b]	
Range	5–6	5–6	
Gender, No. (%)			0.545
F	1 (20)	3 (50)	
M	4 (80)	3 (50)	
Secondary apnea, No. (%)	5 (100)	1 (20)[b]	0.047[a]
Seizures, No. (%)	4 (80)	0 (0)[b]	0.048[a]

There was a significant difference ($p < 0.05$) between the 2 groups for the Apgar score at 1 minute, the initial umbilical arterial pH, and the frequency of secondary apnea and of postnatal seizures. Interestingly, the resuscitation score according to Miller et al[16] was not different between the groups, strengthening the choice of the control group. The data are expressed as median and range, or in some cases ratio and percentage because of the small numbers. Some information such as Apgar score, secondary apnea, and seizures are missing for 1 control case.

[a] $p < 0.05$ statistically significant.

[b] One case is missing information.

[c] According to Miller score.[16]

F = female; HIE = hypoxic–ischemic encephalopathy; M = male.

from Biomol (Enzo Life Sciences, Plymouth Meeting, PA). Protein bands were visualized using the Odyssey Infrared Imaging System (LI-COR, Lincoln, NE). Odyssey v1.2 software (LI-COR) was used for densitometric analysis. Optical density values were normalized with respect to tubulin and expressed as a percentage of values obtained for sham-operated rat pups (100%).

Histochemistry for Lysosomal Enzymes

Histochemistry for acid phosphatase and β-N-acetylhexosaminidase was performed on rat pups perfused intracardially with 2% glutaraldehyde and 1% paraformaldehyde in cacodylate buffer (0.1mol/L, pH 7.4) as previously described.[9]

Electron Microscopy

Electron microscopy was done on rat brains fixed following intracardiac perfusion with 2.5% glutaraldehyde and 2% paraformaldehyde in cacodylate buffer as previously described.[14]

Immunohistochemistry

For rat tissue, pups were perfused intracardially with 4% paraformaldehyde in 0.1mol/l phosphate-buffered saline (PBS), pH 7.4. Immunohistochemistry was performed on 18μm cryostat sections as previously described.[9] For human tissue, the paraffin-embedded sections were first deparaffinized. After antigen retrieval and blocking in PBS with 15% donkey serum, sections were incubated with primary antibodies in 1.5% donkey serum overnight at 4°C.

For both rat and human sections, Alexa Fluor 488 donkey–antirabbit (Invitrogen, Carlsbad, CA; A21206) and Alexa Fluor 594 donkey–antimouse (Invitrogen, A21203) secondary antibodies were incubated and then sections were mounted with FluoroSave (Calbiochem, Darmstadt, Germany; 345–789-20) after a Hoechst staining. An LSM 710 Meta confocal microscope (Carl Zeiss, Oberkochen, Germany) was used for confocal laser microscopy. Confocal images were displayed as individual optical sections. For double labeling, immunoreactive signals were sequentially visualized in the same section with 2 distinct filters, with acquisition performed in separated mode. Images were processed with LSM 710 software and mounted using Photoshop 10.0 (Adobe Systems, San Jose, CA).

The following primary antibodies were used: anti-LC3 (ab48394, for humans) rabbit polyclonal from Abcam, anti–active caspase-3 (9661) rabbit polyclonal from Cell Signaling Technology, anti–cathepsin D (cathD; sc-6486, for humans) goat polyclonal from Santa Cruz Biotechnology, anti–cathB (06–480) and anti–cathD (06–467, for rats) rabbit polyclonal antibody from Upstate Biotechnology (Lake Placid, NY), anti–anti-NeuN (MAB377) mouse monoclonal antibody from Chemicon (Temecula, CA), anti–lysosomal membrane protein 1 (LAMP1; 428017, for rats) from Calbiochem, anti-GFAP (G3893) mouse monoclonal from Sigma, anti-PGP9.5 (7863-0504) rabbit polyclonal from Biotrend (Wangen, Switzerland), and anti-LAMP1 (611042, for humans) mouse monoclonal from BD Biosciences (Franklin Lakes, NJ). Anti-LC3 for rat tissue was a generous gift from Dr Yasuo Uchiyama (Tokyo, Japan).

TUNEL Staining

After an antigen retrieval for paraffin sections or permeabilization (5 minutes in 0.2% Triton-X100) for cryostat sections, TUNEL (terminal deoxynucleotidyl transferase biotin–deoxyuridine triphosphate nick end labeling) staining was performed with the DeadEnd Fluorimetric TUNEL system (Promega, Madison, WI; G3250) according to the manufacturer's instructions. For combined immunolabeling, sections were extensively washed in PBS and incubated in primary and secondary antibodies as described above, except that preincubation of cryostat sections was done without Triton-X100.

Quantification of Autophagic and Lysosomal Labeling

For rat and human thalamus, confocal images of immunocytochemistry against LC3, cathD, cathB, and LAMP1 were acquired using the confocal laser scanning microscope, and images were then processed with Photoshop 10.0. Dots positive for LC3, cathD, cathB, and LAMP1 were quantified using ImageJ (NIH, Bethesda, MD) software and expressed as number of positive dots per neuron per square micrometer. For dots positive for cathD, cathB, and LAMP1, dot areas were also quantified using ImageJ software. To quantify autolysosomal areas, we set a lower limit of $0.5\mu m^2$, in view of the finding that electron microscopical images gave a mean autolysosomal area of $0.58 \pm 0.28\mu m^2$ per neuron.

Statistics

Biological markers data were expressed as mean $\pm$ standard deviation. Rat data were derived from at least 3 independent hypoxic–ischemic experiments, corresponding to at least 3 different litters. Data were analyzed statistically using JMP software (v.10; SAS, Cary, NC). After testing each group of data for distribution normality (using Shapiro–Wilk tests), we used a multivariate analysis of variance (ANOVA) for histochemistry to compare rat sham or human control versus rat HI or human HIE values. For immunoblot, in cases of normal distribution, Welch ANOVA test was followed by a post hoc Tukey–Kramer test. In the case of a non-normal distribution, a Kruskal–Wallis test (nonparametric analog of the 1-way ANOVA) was followed by a post hoc Steel–Dwass test to compare the different time points.

The human descriptive data were expressed as median and range, and analyzed using Statistical Package for Social Science software (v20.0; IBM, Armonk, NY). Univariate analyses of variance, using the Mann–Witney–Wilcoxon and Fisher exact tests, were performed; $p < 0.05$ was chosen as statistically significant.

Results

Perinatal Characteristics of the Human Population

Perinatal data and particularly postnatal adaptation from the 2 groups are represented in the Table.1 There were no statistical differences between the groups for most of the characteristics, such as birth weight, gestational age, and gender. As expected, there were significantly more prenatal sentinel events, reflected by the significantly lower umbilical artery pH and postnatal seizures in the HIE group than in the control group. The time between birth and death was not statistically different in the 2

groups, although the median value was higher in the HIE group. In the control group, the babies died between 1 hour and 28 days after birth (median = 13 hours), whereas in the HIE group, the babies died between 20 hours and 7 days after birth (median = 44 hours).

VLNT of Human Neonates and Ventrobasal Thalamus of Rat Pups Are Highly Vulnerable to HI

In human newborns at term, the predominant neuronal injury pattern after acute and severe asphyxia, known as the "deep nuclear pattern" or "BGT (basal–ganglia–thalamus) pattern," involves the perirolandic cortex, the basal ganglia, the thalamus, and sometimes the brainstem and hippocampus.[19] But the thalamus, and particularly the VLNT, is especially sensitive to HI,[19,20] so we focused on it, and confirmed this sensitivity. In 3 of 5 HIE cases, cerebral MRI (T1 and T2) was performed and showed severe thalamic lesions that were confirmed with diffusion-weighted imaging–ADC as is shown in Figure 1D. Diffusion was severely restricted with ADC levels in the ventrolateral thalamus, ranging from 0.53 to 0.73 $\times$ $10^3 mm^2/s$ (normal values for thalamus = 1.0–1.1 $\times$ $10^3 mm^2/s$). Moreover, hematoxylin and eosin staining revealed pyknotic nuclei and cell shrinkage, confirming neuronal suffering in the VLNT in HIE cases, whereas the control group did not show neuronal injury in the VLNT (see Fig 1E) or in several other gray matter regions (not shown). Similar histological results were observed for the ventrobasal thalamus (VBT) at 24 hours in rat pups in our severe model of neonatal cerebral HI (see Fig 1C).

HI Increases Autophagosome Abundance in Thalamus of Both Rat Pups and Human Newborns

In the neonatal rat model, Western blot analyses of thalamic extracts showed that HI caused an increase in the expression of LC3-II, the lipidated form of LC3, which is a marker of autophagosomal membranes (Fig 2A). Because the LC3-II expression level was highest at 24 hours after HI, we decided to focus our investigations on the 24-hour time point in the rat model.

The effect of HI on autophagy was further investigated by performing immunohistochemistry against LC3. Immunoperoxidase labeling showed a marked increase in the presence of LC3-positive dots (presumably autophagosomes) in the VBT of rats at 6 hours or 24 hours after HI, and to some extent at 72 hours, and in the VLNT of the human HIE cases (see Fig 2). The numbers of LC3-positive dots per neuron were then quantified in confocal images of the VBT of HI rat pups and the VLNT of HIE newborns and compared to counts in sham-operated rats or human control cases, respectively. At 24 hours after HI in rats, the number of LC3-positive dots per neuron was increased by 6-fold compared to sham-operated animals. Similarly, all human HIE cases displayed an up to 10-fold increase in LC3-positive dots compared to control cases, and this was persistent at 7 days (HIE Case 3).

Electron microscopy in HI rat pups revealed that dying VBT neurons displayed marked autophagic characteristics, containing numerous vacuoles, autophagosomes, and autolysosomelike structures in their cytosol (Fig 3). More specifically, the cell death resembled a recently defined kind of autophagic cell death called autosis,[21] which has been shown to involve sequential phases called 1a, 1b, and 2. Each of these phases was represented. Thus, some neurons displayed numerous empty vacuoles, autophagosomes, and autolysosomes (arrowheads) in the cytosol, features representative of autosis phase 1a. In others, parts of the perinuclear space were dilated and contained membrane-bound cytosolic regions, the defining characteristic of phase 1b. Still other dying neurons displayed features of phase 2: gross ballooning of parts of the perinuclear space, and the presence of swollen organelles and rupture of the plasma membrane (see Fig 3B). In addition, these dying neurons also showed some morphological characteristics of apoptosis (chromatin condensation, shrinkage of the cytoplasm) and necrosis (observed in phase 2 autosis such as swelling of organelles). These ultrastructural results thus confirmed that HI induced an increase in autophagosomes in neurons from the rat VBT.

Lysosomal Activity and Autophagic Flux Are Increased following HI in Thalamus of Rat Pups and Human Newborns

To evaluate whether the increased number of autophagosomes was due to enhanced autophagic flux (autophagosome formation and autolysosomal degradation after autophagosome–lysosome fusion) or to failed lysosomal degradation, lysosomal activity was investigated. Immunohistochemistry against different lysosomal markers was performed, and the numbers and sizes of positive dots were quantified. An increased number of lysosomes, especially of very large lysosomes ($>0.5\mu m^2$), which are putatively autolysosomes, would reflect an increase in autophagic flux. In neurons in the thalamus of rat pups and of human newborns, the number of LAMP1-positive vesicles was strongly increased by HI. Moreover, among the positive dots the percentage of larger ones ($>0.5\mu m^2$), which we assume to represent autolysosomes, increased by 12-fold after HI in rats and by 8-fold in

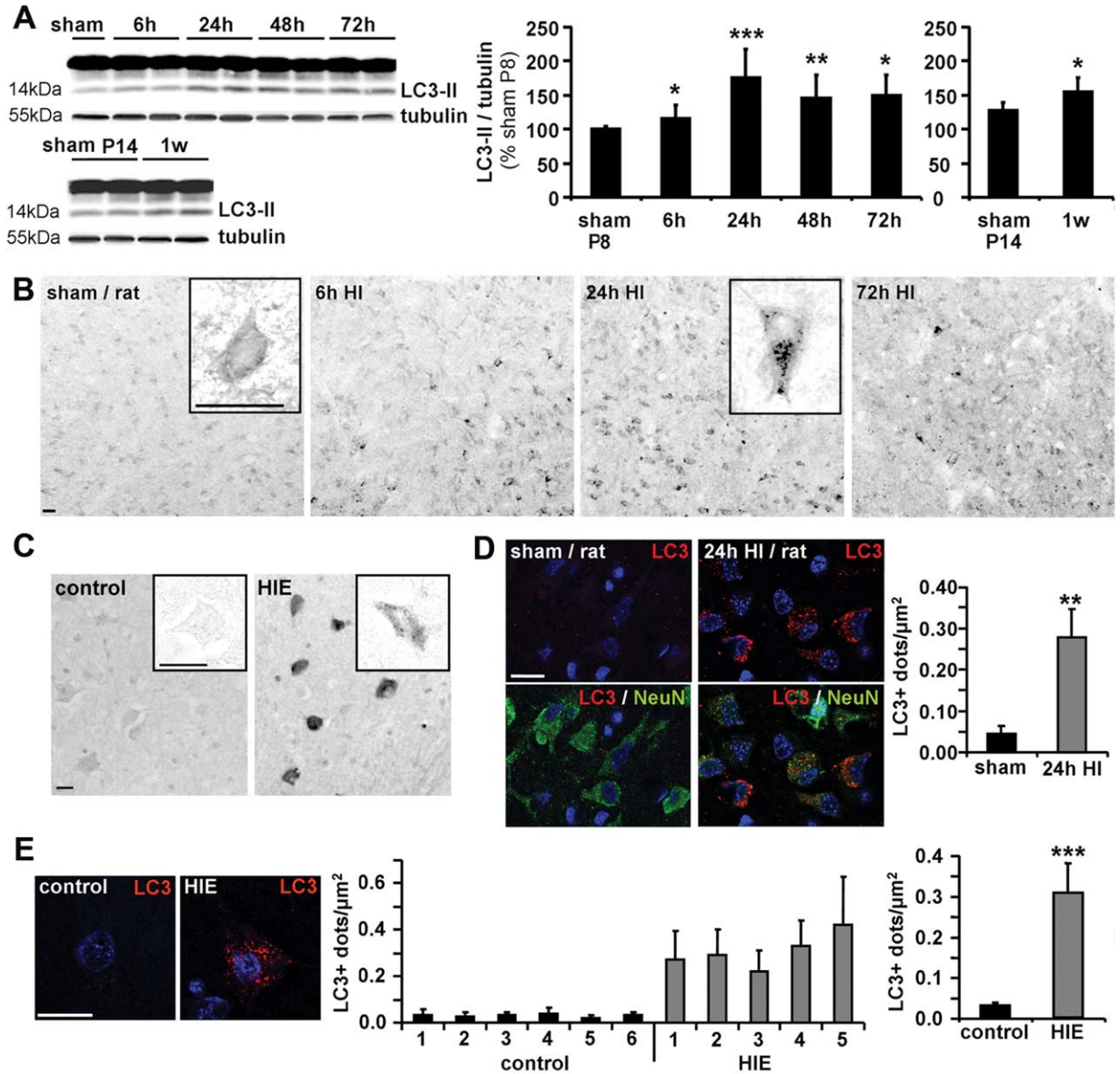

FIGURE 2: Hypoxia–ischemia (HI) increases the number of neuronal autophagosomes in the thalamus of both rat and human neonates. (A) Representative immunoblots and the corresponding quantification of LC3-II expression after HI in rat pups, demonstrating a persistent increase in autophagosomes peaking at 24 hours (6 hours: 116 ± 20%, n = 13; 24 hours: 176 ± 42% n = 16; 48 hours: 146 ± 34%, n = 17; 72 hours: 149 ± 31%, n = 10; 1 week: 156 ± 22%, n = 8) compared to sham-operated animals (sham P8: 100 ± 6%, n = 11; sham P14: 128 ± 11%, n = 7). Values are mean ± standard deviation (SD) and are expressed as a percentage of sham P8 value. Steel–Dwass test: *$p < 0.05$, **$p < 0.01$, ***$p < 0.001$. (B) Representative LC3 immunoperoxidase labeling in the ventrobasal thalamus of rat pups at different time points indicating an increase in LC3-positive dots after HI. High magnifications of a representative neuron in a sham-operated rat and 24 hours after HI are shown. Bars = 20µm. (C) Representative LC3 immunoperoxidase labeling in the ventrolateral thalamus of human newborns illustrating the increase in LC3 expression in hypoxic–ischemic encephalopathy (HIE) cases compared to control. High magnification shows punctate labeling in the HIE case. Bars = 20µm. (D) Representative confocal images of neurons in ventrobasal thalamus of rat pups and quantification of LC3-positive dots (red) in neuronal autophagosomes showing an increase (24 hours HI: 0.278 ± 0.069; sham: 0.046 ± 0.018 LC3-positive dots/neuron/µm^2) at 24 hours after HI. The quantification was performed on neurons labeled with NeuN (green) in 5 rats (20 neurons/rat). Bar = 20µm. (E) Representative confocal images of neurons in ventrolateral thalamus of human newborns, and quantifications. Left graph: numbers of LC3-positive dots in the 6 control and 5 HIE cases shown individually. Right graph: average numbers of LC3-positive dots in control (0.028 ± 0.003) and HIE (0.328 ± 0.035) cases. Bar = 50µm; n ≥ 50 neurons/case. Nuclei are stained with Hoechst (in blue). Values are mean ± SD. Welch analysis of variance: **$p < 0.01$, ***$p < 0.001$.

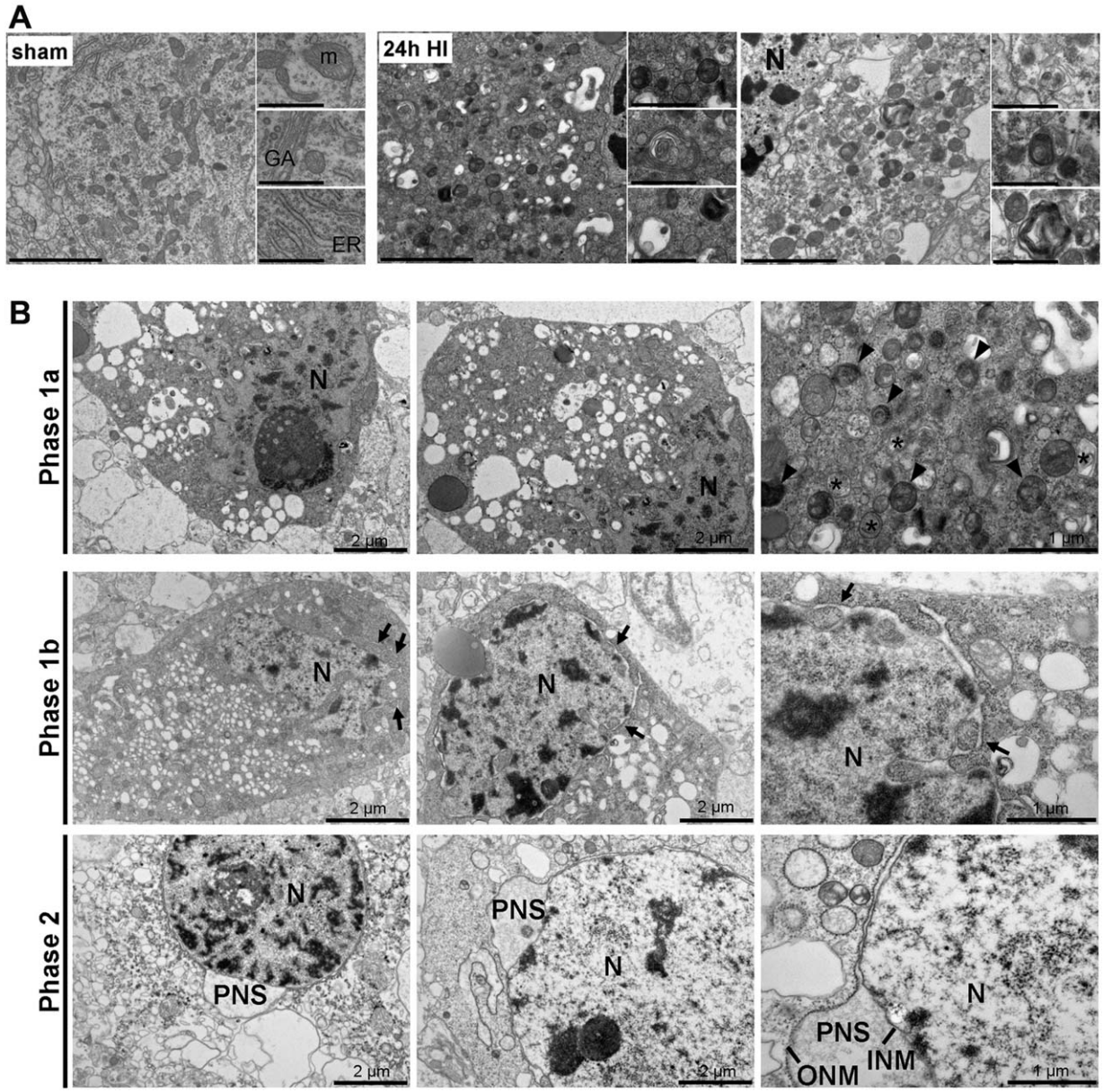

FIGURE 3: Neonatal hypoxia–ischemia (HI)-induced neuronal death in the rat thalamus with autophagic characteristics. (A) Representative electron micrographs of neurons in sham-operated rat pups (right panel) and 24 hours after HI (middle and left panels) showing numerous multimembrane vacuoles (presumably autophagosomes) containing cytoplasmic material as illustrated at high magnifications. Bars = 1μm, 0.5μm for higher magnifications. ER = endoplasmic reticulum; GA = Golgi apparatus; m = mitochondrion; N = nucleus. (B) Electron microscopic analyses revealed that dying neurons in the thalamus showed morphological features of autosis (autophagic cell death). Some dying neurons displayed numerous empty vacuoles, autophagosomes *(asterisks)*, and autolysosomes *(arrowheads)* in the cytosol representative of autosis phase 1a. Others exhibited swollen parts of the perinuclear space containing membrane-bound cytosolic regions (*arrows,* phase 1b). Then, some dying neurons displayed features of phase 2 autosis: focal ballooning of the perinuclear space, swollen organelles, and rupture of the plasma membrane. In addition, these dying neurons also showed some morphological characteristics of apoptosis (chromatin condensation, shrinkage of the cytoplasm) and necrosis (observed in phase 2 autosis such as swelling of organelles). INM = inner nuclear membrane; ONM = outer nuclear membrane; PNS = perinuclear space.

human HIE (Fig 4). Double immunolabeling against LC3 and LAMP1 showed that neurons with a strong punctate LC3 labeling also showed numerous LAMP1-positive vesicles in HI human newborns (see Fig 4E) and rat pups (not shown).

Likewise, immunohistochemistry against the lysosomal protease cathD demonstrated many more cathD-positive dots in HI neurons in both rats (NeuN-positive cells) and humans (PGP9.5-positive cells; Fig 5). Moreover, the size repartition per neuron revealed >34% large

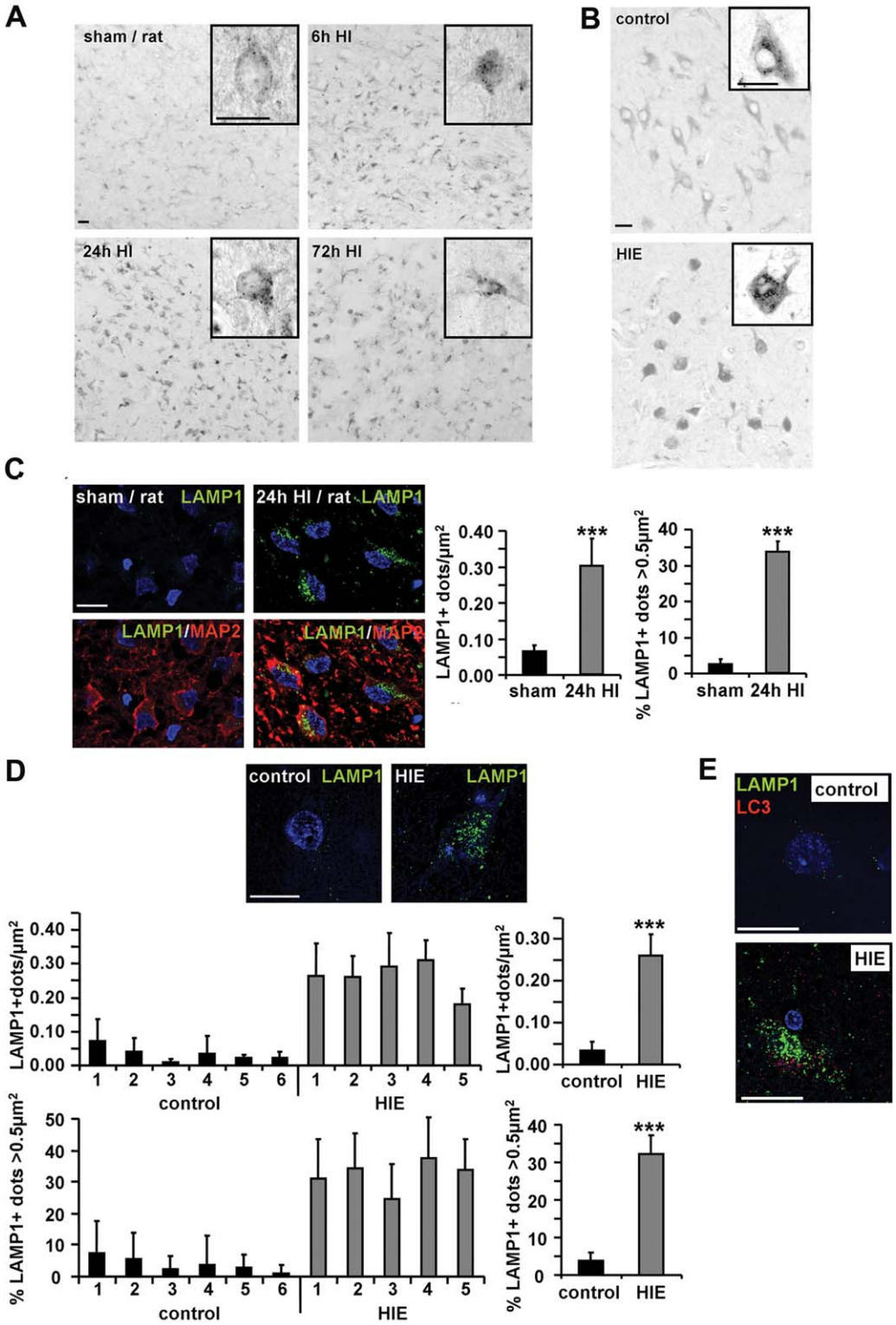

FIGURE 4: Hypoxia-ischemia (HI) in the thalamus of both rat and human neonates increases the number and size of LAMP1-positive vesicles. (A, B) Representative immunoperoxidase labeling of LAMP1 illustrating the increase in its expression after HI in rats (A) and in human hypoxic–ischemic encephalopathy (HIE) cases (B). High magnifications of a representative neuron are shown in each case. At 72 hours after HI, the positive labeling probably corresponds mainly to macrophages, as is suggested by the cellular morphology. Bars = 20μm. (C) Confocal images of LAMP1 expression (green) in neurons labeled with MAP2 (red), near the periphery of the lesion in HI rat pups. Quantification of these data shows increases in the number of dots/neuron/μm^2 (left histogram; sham: 0.065 ± 0.018; 24 hours HI: 0.302 ± 0.077) and in the percentage of large dots with respect to all dots (right histogram; sham: 2.6 ± 1.3%; 24 hours HI: 33.6 ± 3.3%) in rat pups 24 hours after HI; n = 5 rats (20 neurons/rat). (D) A similar analysis showing a strong increase of LAMP1 dots in neurons in human HIE cases. The 2 histograms on the left represent the number of dots/neuron/μm^2 (upper) and the percentage of large dots (>0.5μm^2; lower) in the 6 control and the 5 HIE cases shown individually. The histograms on the right represent the average numbers. Human newborns with severe HIE display far more LAMP1-positive dots (control: 0.033 ± 0.022; HIE: 0.261 ± 0.05) and with a much higher proportion of large vesicles (control: 4.2 ± 1.9%; HIE: 32.2 ± 5%). ***$p < 0.001$. (E) Double immunolabeling against LAMP1 (in green) and LC3 (in red) in human newborn brain sections reveals that in HIE cases neurons with strong autophagic features also display numerous putative autolysosomes (shown by numerous large LAMP1-positive dots). Nuclei are stained with Hoechst (in blue). Bars = 20μm.

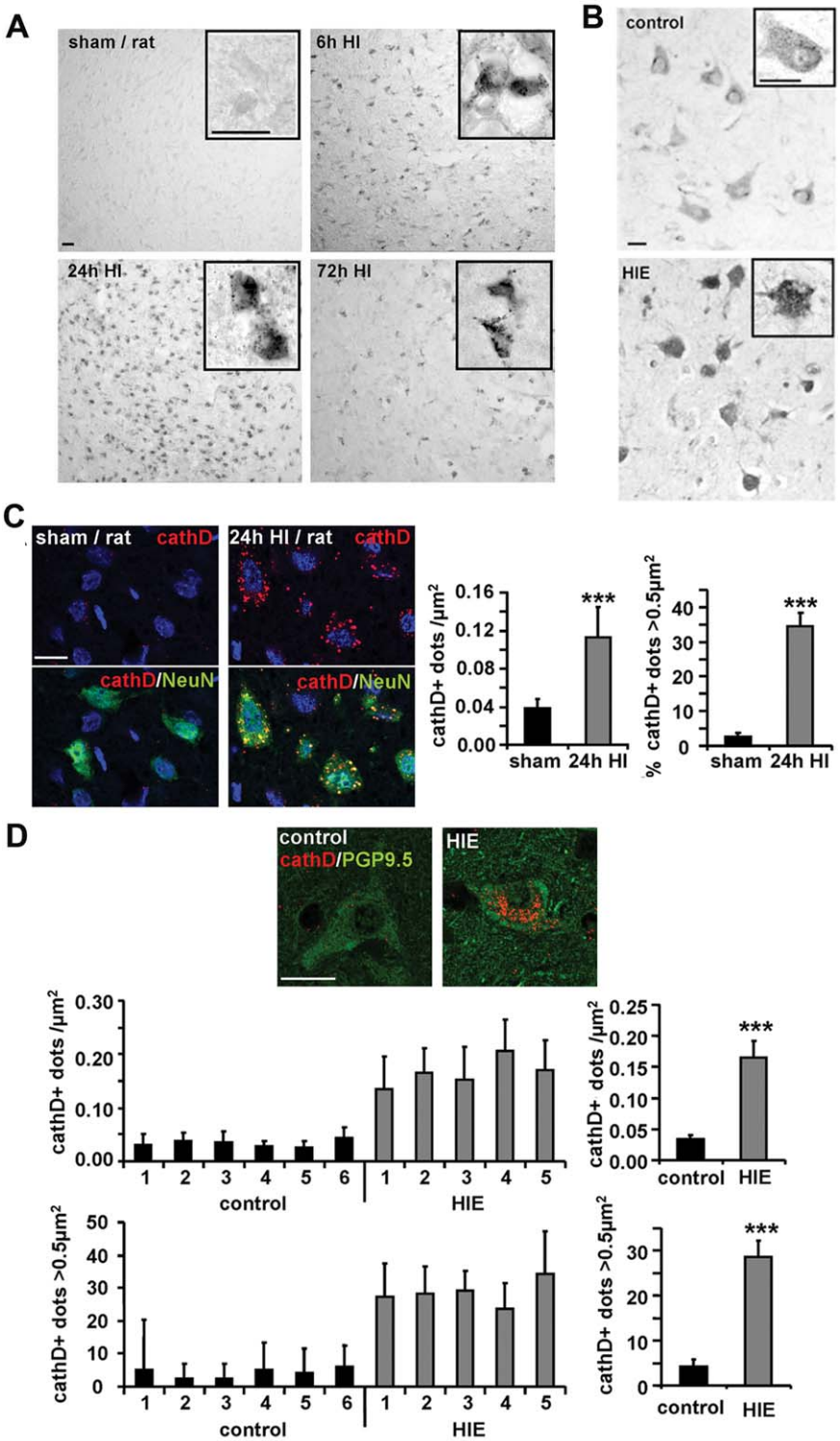

FIGURE 5: Hypoxia–ischemia (HI) in the thalamus of both rat and human neonates increases the number and size of cathepsin D (cathD)-positive vesicles. (A, B) Representative immunoperoxidase labeling of cathD illustrating the increase in cathD expression after HI in rats (A) and in human hypoxic–ischemic encephalopathy (HIE) cases (B). High magnifications of a representative neuron are shown in each case. At 72 hours after HI, the positive labeling probably corresponds mainly to macrophages, as is suggested by the cellular morphology. Bars = 20µm. (C, D) Confocal images of cathD expression (red) in neurons labeled in green with (C) NeuN for rats or (D) PGP9.5 for humans. Quantification of these data shows increases in the numbers of cathD dots. (C) In the rat HI model, the numbers of dots/neuron/µm^2 (upper graph) are 0.039 ± 0.009 for sham and 0.112 ± 0.031 for 24 hours HI. The percentages of dots >0.5µm^2 with respect to all dots are 2.6 ± 1% for sham and 34.4 ± 4% for 24 hours HI. Nuclei are stained with Hoechst (in blue). (D) For human HIE, the 2 histograms on the left represent the number of dots/neuron/µm^2 (upper) and the percentage of large dots with respect to all dots (>0.5µm^2) (lower) in the 6 control and 5 HIE cases shown individually. The 2 histograms on the right represent the average numbers. Human newborns with severe HIE display far more cathD-positive dots (control: 0.033 ± 0.007; HIE: 0.166 ± 0.026) with a much higher proportion of large vesicles (control: 4.3 ± 1%; HIE: 28.6 ± 4%); n ≥ 50 neurons/case. Values are mean ± standard deviation. Welch analysis of variance: ***$p < 0.001$. Bars = 20µm.

dots (>0.5μm^2) after HI in rats and >28% in humans, whereas in controls the percentage was <3% in both rats (see Fig 5C) and humans (see Fig 5D). Immunolabeling for another lysosomal protease, cathB, gave similar results in the rat HI model (data not shown). These results suggest increased lysosomal activity following HI.

To verify this, we studied the activity, rather than merely the expression, of 2 lysosomal enzymes, acid phosphatase (Fig 6A) and β-N-acetylhexosaminidase (see Fig 6B), and found that in each case their activity was enhanced following HI in rat pups, as shown by increased acid phosphatase and β-N-acetylhexosaminidase–positive dots.

To further investigate the change in the level of autophagy, we studied the expression of p62/SQSTM1, a protein selectively degraded by autophagy, by immunoblot on rat extracts.[22] As is shown in Figure 6C, p62 expression was significantly decreased 24 hours after HI. Immunohistochemistry against p62 confirmed the decrease in p62 expression 24 hours after HI in rat pups (see Fig 6D) and also in HI human newborns (see Fig 6E).

Altogether, these results indicate that HI enhances autophagic flux in thalamic neurons in rats and humans.

Enhanced Autophagy in Relation to Neuronal Death in Thalamus of Both Rat Pups and Human Newborns

To investigate the role of the increased neuronal autophagy following HI, we next evaluated the relationships between enhanced autophagy and cell death, focusing on the activation of caspase-3 as a marker of apoptosis and using DNA fragmentation and morphology as additional markers of cell death.

In rat pups, we showed by immunoblotting that cerebral HI increases progressively the expression levels both of cleaved caspase-3 and of the caspase-dependent cleavage product (120kDa) of α-fodrin from 6 hours to at least 72 hours after HI (Fig 7). Immunohistochemistry for cleaved caspase-3 clearly confirmed the activation of caspase-3 in rat VBT, where DNA fragmentation was also detected by TUNEL staining (Fig 8). In human newborns, we likewise showed caspase-3 activation and TUNEL labeling after HI, whereas the controls were always negative for both caspase-3 and TUNEL staining.

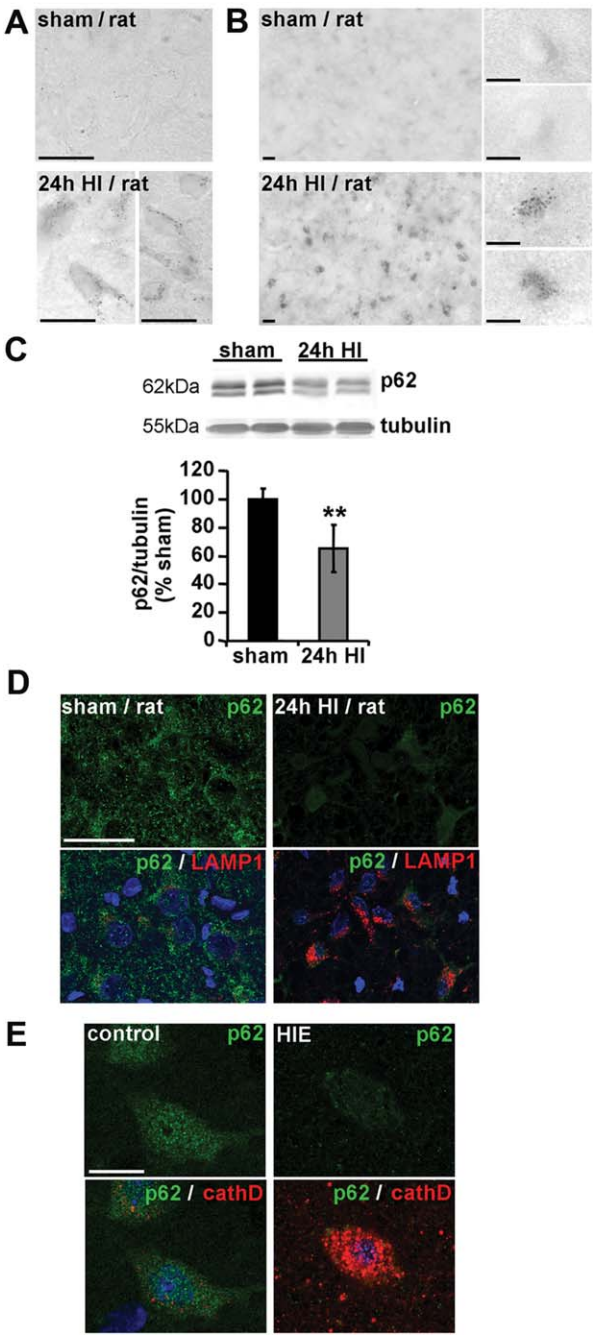

FIGURE 6: Lysosomal activity is enhanced by cerebral hypoxia–ischemia (HI) in the thalamus of both rat and human neonates. Histochemistry for the activity of (A) acid phosphatase and (B) β-N-acetylhexosaminidase shows an increase in the number of positive dots. Bars = 20μm. (C) Representative immunoblots for p62/SQSTM1 and the corresponding quantification, showing that p62 expression in the rat thalamus is significantly reduced 24 hours after HI (sham: 100 ± 7%, n = 9; 24 hours HI: 65 ± 17%, n = 8). Values are mean ± standard deviation and are expressed as a percentage of sham value. Welch analysis of variance: **$p < 0.01$. (D, E) Representative confocal images of p62 (in green) and lysosomal markers (LAMP1 and cathepsin D [cathD] in red) in (D) the rat HI model and (E) human newborns with severe hypoxic–ischemic encephalopathy (HIE) confirming that HI induces a decrease in p62 expression (and no p62 accumulation) in neurons displaying strong autophagic features. Nuclei are stained with Hoechst (in blue). Bars = 20μm.

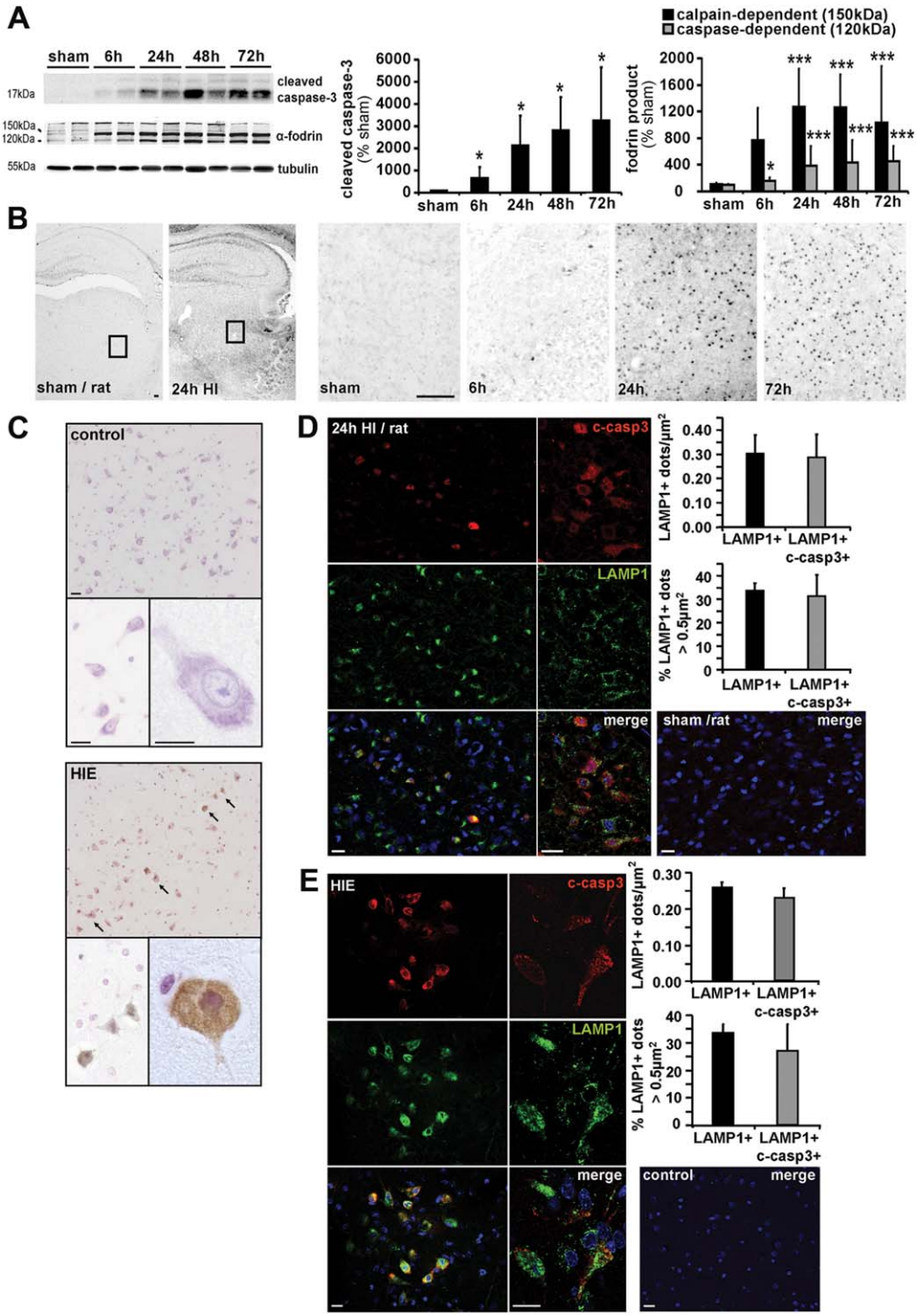

FIGURE 7: Caspase-3 (casp3)-positive neurons are highly autophagic in the thalamus of both rat and human neonates after hypoxia–ischemia (HI). (A) Representative immunoblots for cleaved casp3 and α-fodrin in rat thalamic extracts and the corresponding quantifications demonstrate that HI triggers casp3 activity as shown by an increase in both its cleaved active form (17kDa; 6 hours: 671 ± 477%; 24 hours: 2,135 ± 1,325%; 48 hours: 2,826 ± 1,502%; 72 hours: 3,236 ± 2,430%) and the casp3-dependent cleavage of α-fodrin (120kDa; 6 hours: 153 ± 49; 24 hours: 388 ± 295%; 48 hours: 438 ± 326%; 72 hours: 448 ± 236%; Steel–Dwass test). Immunoblots for α-fodrin also indicate an HI-induced activation of calpains, as suggested by the high level of the calpain-dependent cleavage product (150kDa; 6 hours: 766 ± 487%; 24 hours: 1,268 ± 573%; 48 hours: 1,259 ± 494%; 72 hours: 1,037 ± 841%; Tukey–Kramer test). Values are mean ± standard deviation (SD). $*p<0.05$, $***p<0.001$. (B) Representative images of immunoperoxidase labeling against cleaved casp3 confirm a strong activation of casp3 after HI in the rat ventrobasal thalamus at 6, 24, and 72 hours. (C) Peroxidase immunohistochemistry against cleaved casp3 (in brown) followed by a Nissl stain (in purple) reveals that human hypoxic–ischemic encephalopathy (HIE) brains expressed numerous casp3-positive neurons *(arrows)* with highly condensed and pyknotic nuclei (high magnification) compared to control newborns. Bars = 20μm. (D, E) Confocal images showing LAMP1 (in green) and cleaved casp3 (c-casp3; in red) distribution and the corresponding quantifications illustrating that casp3-positive neurons show a high number of LAMP1-positive dots (upper graph), with a strong proportion of large ones (>0.5μm²; lower graph) in both (D) the ventrobasal thalamus of rat pups 24 hours after HI and (E) the ventrolateral thalamus of human newborns with severe HIE (n = 5). The numbers of LAMP1-positive dots (0.29 ± 0.1 dots/μm² for rats; 0.23 ± 0.09 dots/μm² for humans) and the percentage of dots >0.5μm² (32 ± 9% for rats; 27 ± 10% for humans) per neuron expressing c-casp3 are not significantly different ($p>0.05$) from the average values obtained in overall neurons after HI (0.30 ± 0.08 dots/μm² and 34 ± 3% for rats; 0.26 ± 0.05 dots/μm² and 36 ± 3% for humans). Nuclei are stained with Hoechst (in blue). Values are mean ± SD. Welch analysis of variance was used. n ≥ 20 neurons per rat or per human case. Bars = 20μm.

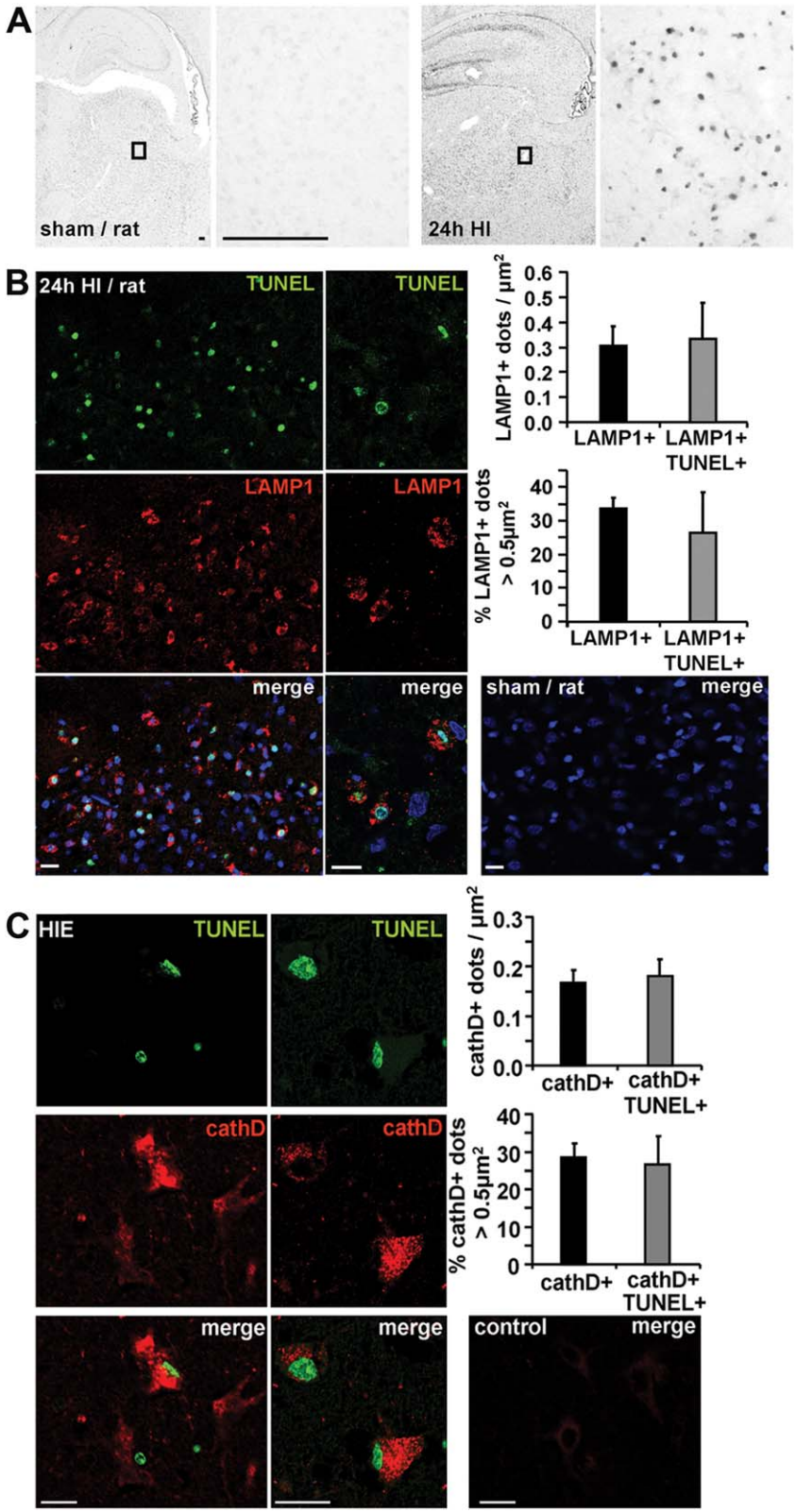

FIGURE 8: TUNEL-positive neurons are highly autophagic in the thalamus of both rat and human neonates after hypoxia–ischemia (HI). (A) Representative images of peroxidase revelation of TUNEL staining following HI demonstrate that neonatal HI strongly increases the number of TUNEL-positive cells at 24 hours after HI. Black rectangles correspond to the higher magnifications in the ventrobasal thalamus. Bar = 100µm. (B) Confocal images of LAMP1 expression (in red) combined with a TUNEL stain (in green) and corresponding quantifications demonstrate that TUNEL-positive neurons of the rat ventrobasal thalamus 24 hours after HI show an increased number of LAMP1-positive dots (upper graph, 0.33 ± 0.14 dots/µm^2) with a strong percentage of large dots (>0.5µm^2; lower graph, $26.43 \pm 12.09\%$) which are not statistically different compared to the overall HI neurons (0.30 ± 0.08 and $34 \pm 3\%$, respectively). Bars = 20µm. Nuclei are stained with Hoechst (in blue). (C) Confocal images showing cathepsin D (cathD; in red) combined with a TUNEL stain (in green) and the corresponding quantifications demonstrating that TUNEL-positive neurons in the ventrolateral thalamus of human newborns show numerous cathD-positive dots (upper graph, 0.18 ± 0.03 dots/µm^2), with a strong proportion of large ones (>0.5µm^2; lower graph, $26.57 \pm 7.45\%$) in severe hypoxic–ischemic encephalopathy ($n = 5$), although the numbers are not statistically different ($p > 0.05$) from the average value obtained in overall neurons after HI (0.16 ± 0.03 dots/µm^2 and $28.57 \pm 3.71\%$, respectively). Values are mean ± standard deviation. Welch analysis of variance was used. $n \geq 20$ neurons/rat or case. Bars = 20µm.

As apoptotic and autophagic processes share several regulators and as autophagy has been shown to trigger caspase-3 activation in cerebral HI, we evaluated the level of autophagy in caspase-3–positive neurons by quantifying the number and size of LAMP1-positive vesicles in rats (see Fig 7D) and humans (see Fig 7E). Double labeling experiments revealed that many thalamic neurons positive for cleaved caspase-3 presented a strong punctate LAMP1 staining, suggesting that the 2 mechanisms occur in the same neurons in HI rats and human HIE brains. Similar results were obtained with TUNEL stain in the rat model 24 hours after HI (see Fig 8B) and in human HIE brains (see Fig 8C).

Altogether, these results reveal that autophagy is enhanced in dying neurons of human VLNT and rat VBT.

Discussion

The present study was designed to investigate the possibility of enhanced neuronal autophagy in severe perinatal HIE in human newborns and to validate the clinical relevance of results obtained by our group and others in experimental HI rodent models. We previously demonstrated that HI in P7 rats enhances neuronal autophagy in CA3 hippocampal and cortical dying neurons.[8,21] Moreover, in a similar HI mouse model, the specific inhibition of autophagy through neuron-specific deletion of the autophagy-related gene *Atg7* conferred resistance to hippocampal neurons,[10] providing a strong argument for a death-mediating role of autophagy in rodent neonatal HI.

Our human brain specimens came from autopsied newborns who died in the context of severe hypoxic–ischemic encephalopathy. It was therefore logical to relate the human results to those from an animal model that is likewise severe. The present neonatal HI rodent model, proposed by Vannucci >30 years ago,[4] has become the standard model and has allowed several deleterious cellular pathways to be identified.[3] One conclusion has been that excitotoxic and HI-induced neuronal death in immature brains occurs across a spectrum ranging from apoptosis to necrosis,[7] but the situation has been complicated by evidence for multiple interacting neuronal death mechanisms,[3,23] including a death-mediating role of enhanced autophagy in different brain regions of neonatal rodents after HI.[8,9,24,25]

Neuronal Autophagy Is Enhanced in Neurons of Human VLNT after HI

We here report for the first time the presence of enhanced autophagy in dying neurons after HI in human newborns. We compared samples to tissues from newborns who died due to other life-incompatible conditions, where no enhanced autophagy could be detected. The main differences between the HIE and the control groups resided in the finding that all HIE cases presented sentinel events affecting them already just before birth. The control group presented a compromised postnatal adaptation due mainly to respiratory insufficiency. Supported by our data from the rat model, we can conclude that autophagic flux, meaning autophagosome formation and autolysosomal degradation, is increased in VLNT human neurons.

First, all HIE cases display an increased number of LC3-positive vesicles compared to control cases. After conjugation to phosphatidylethanolamine, LC3 is converted to the LC3-II form and recruited to the autophagosomal membrane until its degradation by lysosomal hydrolases. Quantification of LC3-positive dots is considered one of the most reliable methods for evaluating autophagosome abundance.[26] Other complementary strategies are the measure of LC3-II expression level after immunoblotting and the identification of multimembrane compartments surrounding cytoplasmic materials including organelles by electron microscopy. The latter two techniques were not possible on the human brain samples but were performed on rat pup brains, confirming that neonatal HI increases autophagosomal numbers in the rat VBT.

To confirm an enhanced autophagic flux, it is essential to demonstrate that increased autophagosome abundance occurs along with a higher level of lysosomal clearing, because a defect in degradation would result in autophagosome accumulation. After human and rat neonatal HI, lysosomal vesicles labeled with LAMP1, cathD, and/or cathB were not only more numerous but also larger in thalamic neurons containing abundant autophagosomes (LC3-positive dots), indicating greater autophagic lysosomal activity with increased presence of autolysosomes. This hypothesis was strengthened by our results in the rat model showing degradation of the autophagy substrate p62 and enhanced activity of 2 lysosomal enzymes in VBT after HI. In both rat and human thalamic neurons, p62 immunolabeling confirmed that p62 was apparently reduced and certainly not accumulated following HI. Several studies have shown enhanced neuronal autophagy in diverse in vitro[27,28] and in vivo[29,30] models of excitotoxicity, including adult and neonatal cerebral HI.[9,10,13,14,31–35]

Enhanced Autophagy Occurs in Dying Neurons of Human VLNT after HI

Our results also show, in both humans and rats, that many of the neurons expressing enhanced autophagy were dying, because many of them were positive for activated caspase-3 and for TUNEL. In humans, very few

postmortem neuropathological studies of neonatal HIE are available, and most described only necroticlike cell death,[36] although a few did mention the presence of apoptosis in the cerebral cortex and basal ganglia.[3] Our results make it clear that apoptoticlike cell death with apoptotic (but also necrotic) features including caspase-3 activation did occur in VLNT. This was yet another point of resemblance between the human and the rodent neuropathologies. Several rodent studies have described related results in cerebral ischemia in both adults[29,31,34] and neonates.[9,10] However, in our neonatal HI rat model the relationships with apoptosis can be region-dependent, because strong autophagy is activated simultaneously with apoptosis in cortical neurons, whereas in the degenerating hippocampus CA1 neurons are purely apoptotic (not autophagic) and CA3 neurons are purely autophagic (not apoptotic).[9] The neuronal cell death induced by HI in the thalamus of rat pups is thus more comparable to that occurring in the cortex. In such cases, with autophagy and apoptosis activated in the same neuron, the autophagy may perhaps trigger an apoptotic execution, as has been shown in the death of cortical neurons exposed to different apoptotic stimulations.[18]

Both human and animal studies have demonstrated sexual dimorphism in neonatal cerebral HI.[37–40] It has been shown that there is sex-specific activation of cell death signaling pathways. For example, cell death in females occurs mainly via a caspase-dependent pathway, whereas in males caspase-independent pathways (apoptosis-inducing factor [AIF], poly[adenosine diphosphate ribose] polymerase) seem to be more important players.[41–43] We currently work only with male rat pups to avoid any possible gender differences in signaling. However, in the human data we were obliged to use both genders because of the scarcity of available brain tissue. However, when the HI insult is severe in rodents, there are no significant sex differences in the extent of brain damage[41] (see Fig 1B) or in the level of LC3-II expression (not shown).[41]

We did not, however, address the function of the neuronal autophagy in the present study. Enhanced autophagy can be related to cell death in different ways. Its best known function is a protective reaction to maintain cell survival, as has been described in nutrient deprivation or pathogen invasion.[44–46] It can also be just an epiphenomenon or, at the other extreme, an active player in the cell death machinery. Evidence for a detrimental role in cerebral ischemia is currently much stronger than that for a protective one.[23] In particular, strong evidence for a death-promoting role of autophagy has been deduced in several cerebral ischemia models from the neuroprotective effects of its inactivation, achieved not only by pharmacological means in numerous papers,[11,14,47] but also by the specific knockdown of autophagy genes in adult cerebral ischemia[35] or their specific deletion in a conditional knockout model of neonatal HI.[10] We recently demonstrated that downregulation of the autophagy-related protein beclin1 reduced the striatal lesion in the same hypoxic–ischemic rodent model as in the present experiments.[48] Our data corroborate the study of Koike and colleagues showing that the hippocampus becomes resistant in mice when another autophagy-related gene, *Atg7*, is specifically inhibited in neurons after mild HI.[10] Moreover, we recently showed that cardiac glycosides such as neriifolin were able to inhibit a form of autophagic cell death, designated autosis, that occurs in the present model.[21] Our present results indicate that the neuronal death in the thalamus resembles autosis but has features of apoptosis as well. Of particular interest, neonatal hypoxic–ischemic brain damage and autophagy in rats were both strongly reduced by treatment with neriifolin in both cortex and thalamus.[21] In cases where neuronal enhanced autophagy promotes cell death, the cellular pathways involved can be various. It can trigger necrosis[49,50] but more often apoptosis.[18,51–53] We previously demonstrated that some widely used apoptotic stimuli can activate autophagy flux in primary cortical neurons with a strong contribution to caspase-dependent (caspase-3 activation) and caspase-independent (AIF nuclear translocation) apoptosis.[18] In specific conditions, autophagy can also be a cell death mechanism by itself, independently of apoptosis or necrosis.[12,19,54–56] Due to its described paradoxical roles, the function of enhanced autophagy in cell death is still a subject of debate.[12,57]

In conclusion, we have shown for the first time that autophagy is enhanced in thalamic neurons of human newborns with HIE as well as in a rodent model of severe perinatal asphyxia. We hypothesize, based on experimental results on different rodent models of cerebral ischemia, that autophagy could be involved in triggering neuronal death in the human HIE. Experimental neuroprotective strategies targeting autophagy could then be a promising lead to follow for the development of future therapeutic approaches.

Acknowledgment

This research was supported by grants from the Swiss National Science Foundation (310030-130769), Emma Muschamp Foundation, and Faculty of Biology and Medicine (University of Lausanne).

We thank J. Daraspe of the Electron Microscopy Facility (University of Lausanne) and Cellular Imaging

Facility (University of Lausanne) for technical and experimental support, and Dr C. Fischer for statistical analysis of the human data.

This work is dedicated to Dr Maria Delivoria-Papadopoulos in thanks for her tremendous mentoring of A.C.T.

Authorship

All authors have contributed substantially to this research study. V.G. performed experiments on animal and human tissue, analysis of the data, and wrote much of the manuscript. M.P.P. performed experiments on human tissue, analyzed the data, and wrote much of the manuscript. C.R. performed parts of experiments. M.C.O. participated in selecting human tissue and revised the manuscript. R.M. participated in description and analysis of the magnetic resonance images of the newborns and revised the manuscript. P.G.H.C. helped in designing the study and revised the manuscript. J.P. and A.C.T. designed and supervised the experiments and were involved in the writing of the manuscript. V.G. and M.P.P. contributed equally as co-first authors. J.P. and A.C.T. contributed equally as co-last authors.

Potential Conflicts of Interest

Nothing to report.

References

1. Edwards AD, Brocklehurst P, Gunn AJ, et al. Neurological outcomes at 18 months of age after moderate hypothermia for perinatal hypoxic ischaemic encephalopathy: synthesis and meta-analysis of trial data. BMJ 2010;340:c363.
2. Okereafor A, Allsop J, Counsell SJ, et al. Patterns of brain injury in neonates exposed to perinatal sentinel events. Pediatrics 2008; 121:906–914.
3. Northington FJ, Chavez-Valdez R, Martin LJ. Neuronal cell death in neonatal hypoxia-ischemia. Ann Neurol 2011;69:743–758.
4. Rice JE, Vannucci RC, Brierley JB. The influence of immaturity on hypoxic-ischemic brain-damage in the rat. Ann Neurol 1981;9: 131–141.
5. Romijn HJ, Hofman MA, Gramsbergen A. At what age is the developing cerebral cortex of the rat comparable to that of the full-term newborn human baby? Early Hum Dev 1991;26:61–67.
6. Northington FJ. Brief update on animal models of hypoxic-ischemic encephalopathy and neonatal stroke. ILAR J 2006;47: 32–38.
7. Portera-Cailliau C, Price DL, Martin LJ. Excitotoxic neuronal death in the immature brain is an apoptosis-necrosis morphological continuum. J Comp Neurol 1997;378:70–87.
8. Northington FJ, Ferriero DM, Graham EM, et al. Early neurodegeneration after hypoxia-ischemia in neonatal rat is necrosis while delayed neuronal death is apoptosis. Neurobiol Dis 2001;8: 207–219.
9. Ginet V, Puyal J, Clarke PGH, et al. Enhancement of autophagic flux after neonatal cerebral hypoxia-ischemia and its region-specific relationship to apoptotic mechanisms. Am J Pathol 2009; 175:1962–1974.
10. Koike M, Shibata M, Tadakoshi M, et al. Inhibition of autophagy prevents hippocampal pyramidal neuron death after hypoxic-ischemic injury. Am J Pathol 2008;172:454–469.
11. Puyal J, Ginet V, Grishchuk Y, et al. Neuronal autophagy as a mediator of life and death: contrasting roles in chronic neurodegenerative and acute neural disorders. Neuroscientist 2012;18:224–236.
12. Clarke PGH, Puyal J. Autophagic cell death exists. Autophagy 2012;8:867–869.
13. Zhu C, Wang X, Xu F, et al. The influence of age on apoptotic and other mechanisms of cell death after cerebral hypoxia-ischemia. Cell Death Differ 2005;12:162–176.
14. Puyal J, Vaslin A, Mottier V, et al. Postischemic treatment of neonatal cerebral ischemia should target autophagy. Ann Neurol 2009;66:378–389.
15. Sarnat HB, Sarnat MS. Neonatal encephalopathy following fetal distress—clinical and electroencephalographic study. Arch Neurol 1976;33:696–705.
16. Miller SP, Weiss J, Barnwell A, et al. Seizure-associated brain injury in term newborns with perinatal asphyxia. Neurology 2002; 58:542–548.
17. Rutherford M, Biarge MM, Allsop J, et al. MRI of perinatal brain injury. Pediatr Radiol 2010;40:819–833.
18. Grishchuk Y, Ginet V, Truttmann AC, et al. Beclin 1-independent autophagy contributes to apoptosis in cortical neurons. Autophagy 2011;7:1115–1131.
19. de Vries LS, Groenendaal F. Patterns of neonatal hypoxic-ischaemic brain injury. Neuroradiology 2010;52:555–566.
20. Krageloh-Mann I, Helber A, Mader I, et al. Bilateral lesions of thalamus and basal ganglia: origin and outcome. Dev Med Child Neurol 2002;44:477–484.
21. Liu Y, Shoji-Kawata S, Sumpter RM Jr, et al. Autosis is a Na+,K+-ATPase-regulated form of cell death triggered by autophagy-inducing peptides, starvation, and hypoxia-ischemia. Proc Natl Acad Sci U S A 2013;110:20364–20371.
22. Ichimura Y, Kumanomidou T, Sou YS, et al. Structural basis for sorting mechanism of p62 in selective autophagy. J Biol Chem 2008;283:22847–22857.
23. Puyal J, Ginet V, Clarke PGH. Multiple interacting cell death mechanisms in the mediation of excitotoxicity and ischemic brain damage: a challenge for neuroprotection. Prog Neurobiol 2013; 105:24–48.
24. Nakajima W, Ishida A, Lange MS, et al. Apoptosis has a prolonged role in the neurodegeneration after hypoxic ischemia in the newborn rat. J Neurosci 2000;20:7994–8004.
25. Sheldon RA, Hall JJ, Noble LJ, et al. Delayed cell death in neonatal mouse hippocampus from hypoxia-ischemia is neither apoptotic nor necrotic. Neurosci Lett 2001;304:165–168.
26. Klionsky DJ, Abdalla FC, Abeliovich H, et al. Guidelines for the use and interpretation of assays for monitoring autophagy. Autophagy 2012;8:445–544.
27. Borsello T, Croquelois K, Hornung JP, et al. N-methyl-D-aspartate-triggered neuronal death in organotypic hippocampal cultures is endocytic, autophagic and mediated by the c-Jun N-terminal kinase pathway. Eur J Neurosci 2003;18:473–485.
28. Matyja E, Taraszewska A, Naganska E, et al. Autophagic degeneration of motor neurons in a model of slow glutamate excitotoxicity in vitro. Ultrastruct Pathol 2005;29:331–339.
29. Piras A, Gianetto D, Conte D, et al. Activation of autophagy in a rat model of retinal ischemia following high intraocular pressure. Plos One 2011;6:e22514.

30. Shacka JJ, Lu J, Xie ZL, et al. Kainic acid induces early and transient autophagic stress in mouse hippocampus. Neurosci Lett 2007;414:57–60.

31. Adhami F, Liao GH, Morozov YM, et al. Cerebral ischemia-hypoxia induces intravascular coagulation and autophagy. Am J Pathol 2006;169:566–583.

32. Gao L, Jiang T, Guo J, et al. Inhibition of autophagy contributes to ischemic postconditioning-induced neuroprotection against focal cerebral ischemia in rats. Plos One 2012;7:e46092.

33. Nitatori T, Sato N, Kominami E, et al. Participation of cathepsins B, H, and L in perikaryal condensation of CA1 pyramidal neurons undergoing apoptosis after brief ischemia. Adv Exp Med Biol 1996;389:177–185.

34. Rami A, Langhagen A, Steiger S. Focal cerebral ischemia induces upregulation of beclin 1 and autophagy-like cell death. Neurobiol Dis 2008;29:132–141.

35. Xing SH, Zhang YS, Li JJ, et al. Beclin 1 knockdown inhibits autophagic activation and prevents secondary neurodegenerative damage in the ipsilateral thalamus following focal cerebral infarction. Autophagy 2012;8:63–76.

36. Takizawa Y, Takashima S, Itoh M. A histopathological study of premature and mature infants with pontosubicular neuron necrosis: neuronal cell death in perinatal brain damage. Brain Res 2006; 1095:200–206.

37. Alkayed NJ, Harukuni I, Kimes AS, et al. Gender-linked brain injury in experimental stroke. Stroke 1998;29:159–165.

38. Hurn PD, Vannucci SJ, Hagberg H. Adult or perinatal brain injury—does sex matter? Stroke 2005;36:193–195.

39. Vagnerova K, Koerner IP, Hurn PD. Gender and the injured brain. Anesth Analg 2008;107:201–214.

40. Turtzo LC, McCullough LD. Sex-specific responses to stroke. Future Neurol 2010;5:47–59.

41. Zhu CL, Xu FL, Wang XY, et al. Different apoptotic mechanisms are activated in male and female brains after neonatal hypoxia-ischaemia. J Neurochem 2006;96:1016–1027.

42. Lang JT, McCullough LD. Pathways to ischemic neuronal cell death: are sex differences relevant? J Transl Med 2008;6:33.

43. Renolleau S, Fau S, Charriaut-Marlangue C. Gender-related differences in apoptotic pathways after neonatal cerebral ischemia. Neuroscientist 2008;14:46–52.

44. Kuma A, Hatano M, Matsui M, et al. The role of autophagy during the early neonatal starvation period. Nature 2004;432:1032–1036.

45. Liang XH, Kleeman LK, Jiang HH, et al. Protection against fatal Sindbis virus encephalitis by beclin, a novel Bcl-2-interacting protein. J Virol 1998;72:8586–8596.

46. Mizushima N. Role of mammalian autophagy as a starvation response. Mol Biol Cell 2004;15:242A.

47. Wen YD, Sheng R, Zhang LS, et al. Neuronal injury in rat model of permanent focal cerebral ischemia is associated with activation of autophagic and lysosomal pathways. Autophagy 2008;4:762–769.

48. Ginet V, Spiehlmann A, Rummel C, et al. Involvement of autophagy in hypoxic-excitotoxic neuronal death. Autophagy 2014;10: 846–860.

49. Samara C, Syntichaki P, Tavernarakis N. Autophagy is required for necrotic cell death in Caenorhabditis elegans. Cell Death Differ 2008;15:105–112.

50. Wang JY, Xia QA, Chu KT, et al. Severe global cerebral ischemia-induced programmed necrosis of hippocampal CA1 neurons in rat is prevented by 3-methyladenine: a widely used inhibitor of autophagy. J Neuropathol Exp Neurol 2011;70:314–322.

51. Dong XX, Wang YR, Qin S, et al. P53 mediates autophagy activation and mitochondria dysfunction in kainic acid-induced excitotoxicity in primary striatal neurons. Neuroscience 2012;207: 52–64.

52. Xue LZ, Fletcher GC, Tolkovsky AM. Autophagy is activated by apoptotic signalling in sympathetic neurons: an alternative mechanism of death execution. Mol Cell Neurosci 1999;14:180–198.

53. Zhang XD, Wang Y, Wang Y, et al. p53 mediates mitochondria dysfunction-triggered autophagy activation and cell death in rat striatum. Autophagy 2009;5:339–350.

54. Clarke PGH. Developmental cell death: morphological diversity and multiple mechanisms. Anat Embryol (Berl) 1990;181:195–213.

55. Denton D, Shravage B, Simin R, et al. Autophagy, not apoptosis, is essential for midgut cell death in drosophila. Curr Biol 2009;19: 1741–1746.

56. Luciani MF, Giusti C, Harms B, et al. Atg1 allows second-signaled autophagic cell death in Dictyostelium. Autophagy 2011;7:501–508.

57. Kroemer G, Levine B. Autophagic cell death: the story of a misnomer. Nat Rev Mol Cell Biol 2008;9:1004–1010.